Impacts of interruption of the Agulhas leakage on the tropical Atlantic in coupled ocean-atmosphere simulations

Reindert J. Haarsma[1], Edmo J. D. Campos[2], Sybren Drijfhout[1], Wilco Hazeleger[1], and Camiel Severijns[1]

[1]Royal Netherlands Meteorological Institute (KNMI), Netherlands
[2]Oceanographic Institute, University of São Paulo (IOUSP), Brazil

Corresponding author:

Reindert J. Haarsma
Royal Netherlands Meteorological Institute
P.O. Box 201
3730 AE De Bilt,
The Netherlands
haarsma@knmi.nl

Accepted for publication in Climate Dynamics

October 2009

ABSTRACT

In this paper we use a coupled ocean-atmosphere model to investigate the impact of the interruption of Agulhas leakage of Indian ocean water on the Tropical Atlantic, a region where strong coupled ocean atmosphere interactions occur. The effect of a shut down of leakage of Indian ocean water is isolated from the effect of a collapse of the MOC. In our experiments, the ocean model is forced with boundary conditions in the southeastern corner of the domain that correspond to no interocean exchange of Indian ocean water into the Atlantic. The southern boundary condition is taken from the Levitus data and ensures a MOC in the Atlantic. Within this configuration, instead of warm and salty Indian ocean water temperature (cold) and salinity (fresh) anomalies of southern ocean origin propagate into the South Atlantic and eventually reach the equatorial region, mainly in the thermocline. This set up mimics the closure of the “warm water path” in favor of the “cold water path”. As part of the atmospheric response, there is a northward shift of the Intertropical Convergence Zone (ITCZ). The changes in Trade Winds lead to reduced Ekman pumping in the equatorial region. This leads to a freshening and warming of the surface waters along the equator. Especially in the Cold Tongue region, the cold and fresh subsurface anomalies do not reach the surface due to the reduced upwelling. The anomaly signals are transported by the Equatorial undercurrent and spread away from the Equator within the thermocline. Part of the anomaly eventually reaches the Tropical North Atlantic, where it affects the Guinea Dome. Surprisingly, the main effect at the surface is small on the equator and relatively large at the Guinea Dome. In the atmosphere, the northward shift of the ITCZ is associated with a band of negative precipitation anomalies and higher salinities over the Tropical South Atlantic. An important implication of these results is that the modified water characteristics due to a shut down of the Agulhas leakage remain largely unaffected when crossing the equatorial Atlantic and therefore can affect the deepwater formation in the North Atlantic. This supports the hypothesis that the Agulhas leakage is an important source region for climate change and decadal variability of the Atlantic.

1. Introduction

The South Atlantic is a peculiar ocean. It is the only basin wherein the net meridional heat flux is equatorward in subtropical regions, resulting in cross-equatorial export of heat towards the Northern Hemisphere. This inter-hemispheric heat transport requires a northward cross-equatorial mass flux in the upper layers, which is compensated by the southward transport of North Atlantic Deep Water (NADW) in the lower layers. The north-south trade of water in the Atlantic is a widely known part of the global thermohaline circulation (THC). Nonetheless, some intriguing questions still remain on the origins of the water masses crossing the equator in the upper layers, their relative importance and what are the main routes followed by them. It is well accepted today that the upper limb of this Atlantic meridional overturning circulation (MOC) receives inflows from the Pacific, through the Drake Passage, and from the Indian Ocean. The Indian Ocean contribution occurs by means of the water mass transported by rings and filaments at the Agulhas retroflection, usually referred as the Agulhas leakage, and feeds into the subtropical South Atlantic waters relatively warmer and saltier, as compared to those coming from the Pacific, through the Drake Passage. An interruption of this water pathway would certainly have some consequences for the Atlantic MOC, as suggested by Peeters (2004), who provided paleo evidence for the impact of Agulhas leakage on MOC. Ocean-only model simulations by Biastoch et al. (2008) also indicate that on decadal time scale the MOC is affected by variations in Agulhas leakage.

Studies with coupled climate models have investigated the impact of major changes in the MOC on the atmospheric and oceanic circulation on a global scale. With respect to changes in the climatology, Vellinga and Wood (2002), Dahl et al. (2005), and Haarsma et al. (2008) (HET2008) found that a weakened MOC results in a dipole response over the Atlantic, with a cooling in the North Atlantic and a warming in the tropical and South Atlantic. Similar results were found by Zhang and Delworth (2005), together with a significant El Niño-like response in the tropical Pacific and a southward shift of the inter tropical convergence zone (ITCZ) over the Atlantic and Pacific. Recently Chang et al. (2008) suggested that the warming of the equatorial South Atlantic is due to the reverse of the subsurface North Brazil Current (NBC) thereby advecting warm equatorial North Atlantic subsurface waters into the equatorial South Atlantic. These modeling results appear to be supported by paleo-records (Stott et al. 2002, Peterson et al. 2000). Because the seasonal cycle and the interannual

variability are strongly linked to the climatological mean state, it is expected that they also will be affected by a weakened MOC. The changes in the seasonal cycle and interannual variability might be profound and exceed the changes in the mean state.

Indeed, HET2008 showed that the seasonal cycle, as well as the interannual variability in sea surface temperature (SST), are reduced because the tropical thermocline is deepened, especially in the east. As a result, the characteristics of the cold tongue mode, which is the dominant mode of variability along the Equator (Xie and Carton 2004), are changed: the variability in the eastern equatorial region is strongly reduced and the largest variability is now in the Benguela region. The gradient mode, which is the dominant mode of variability in the subtropical North Atlantic (Xie and Carton 2004), remains unaltered. The warming of the tropical Atlantic enhances and shifts the Hadley circulation.

Using a high resolution ocean model and a Lagrangian tracking technique Hazeleger et al. (2003b) showed that the Equatorial undercurrent (EUC) is ventilated from the south. In addition, Hazeleger and Drijfhout (2006) showed, using the same technique, that the MOC affects the subtropical cells (STC), and that MOC water recirculates in the tropics. From this result they concluded that the MOC can substantially affect the tropical circulation. This suggests that not only a collapse of the MOC, but also a change in the characteristics of the MOC water would affect the tropical climate. The characteristics of the MOC water are modified in crossing the tropical Atlantic and this will determine how the shut down of Agulhas leakage of Indian ocean water will affect the deep-water formation in the North Atlantic and the strength of the MOC.

The collapse of the MOC in a coupled model is usually accomplished by a massive perturbation of the salinity of the Atlantic ocean. Perturbations in the Agulhas leakage have not been performed in coupled simulations. Here we address the question of what happens when Agulhas leakage is replaced by waters from Southern Ocean origin. An important question is, how the characteristics of water masses change along the pathway from the Southern Atlantic to the regions of deep-water formation in the North Atlantic. The tropical Atlantic is an upwelling region. Due to interaction with the atmosphere the characteristics of the water masses can strongly be modified when crossing the equatorial region. This process could delay and diminish the impact of a shut down of the Agulhas leakage. Additional questions are related to the time scale of the crossing of the Atlantic and the pathways of the modified water masses. In this study we have investigated these questions using a global atmosphere model coupled to a regional ocean model of the Atlantic basin. The MOC is

maintained at the strength of 20 Sv by relaxing to prescribed temperature and salinity profiles at the northern and southern boundary of the ocean model. In our numerical experiments a shut down of the Agulhas leakage of Indian ocean water is simulated by replacing the eastern boundary conditions south of the southern tip of Africa by those from from a global ocean simulation in which there is no influx from the Indian Ocean, due to a collapse of the MOC. Because the southern boundary conditions are not changed the strength of the MOC is not affected, but cooler and fresher thermocline water of Southern Ocean origin is now advected into the South Atlantic. This experimental set-up mimics a shift from inflow via the warm water path to an inflow via the cold water path (Gordon 1986, Rintoul 1991).

The model used here is the Speedy-MICOM implementation used by Hazeleger and Haarsma, (2005) (HH2005) and (HET2008). Differently from other state-of-the-art coupled models which do not simulate realistic tropical Atlantic climate and variability (Breugem et al. 2007), this regionally coupled model is well suited to study the response of the Tropical Atlantic, because it is able to simulate realistically the tropical Atlantic climate and variability. This occurs, as for the regional model the SSTs outside the Atlantic are prescribed, which limits the possibility of the model to deviate globally from the observed climate. In addition the model is especially tuned to simulate the tropical Atlantic climate and variability. The main tuning parameters were the entrainment due to wind mixing, and the parameterization of stratiform clouds (HH2005).

In Section 2 we describe the model and the set-up of the experiments. The results are presented and discussed in Section 3. The conclusions are shown in Section 4.

2. Methodology

2.1 The Model

The coupled Speedy-MICOM model (Hazeleger et al. 2003a) is the same as used in HH2005 and HET2008 and will only briefly be described here. It consists of an atmospheric primitive equation model (Speedy) with a vertical resolution of seven layers and a triangular spectral truncation at total wavenumber 30 (T30). The model has simplified physics which makes it computationally inexpensive. A five-layer version is described in detail by Molteni (2003). The ocean component is the 2.7 version of the Miami Isopycnic Coordinate Ocean

Model (MICOM), described by Bleck et al. (1992). This model uses potential density as vertical coordinate. In our simulations, it is configured with 19 layers and has a horizontal resolution of 1 degree. The domain is the Atlantic basin from 40^{o} S to 60^{o} N. Restoring boundary conditions of the thermodynamic properties, taken from the Levitus (1998)) data, are applied at the northern and southern lateral boundaries. To avoid discontinuities the relaxation is not only applied at the boundaries but up to two grid point distances into the interior of the basin. The relaxation timescale varies from 5 days at the boundary to 30 days for the second point into the interior. The relaxation profiles follow an annual cycle. Outside the Atlantic basin and over land, climatological surface temperatures are prescribed. In HH2005 it is shown that for present-day conditions Speedy-MICOM reproduces well the tropical Atlantic climatology, including the east-west tilt of the thermocline along the equator. For most of the tropical Atlantic the error in SST is less than 2^{o}C. As a result, Speedy-MICOM simulates realistically the tropical Atlantic variability including the gradient mode and the cold tongue mode. This enables us to investigate the response of the tropical Atlantic climate when water masses with different characteristics enter the equatorial region.

2.2 The Experiments

Two simulations were made: a control run (CONTROL), representing present-day conditions, and an experiment in which the Agulhas leakage of Indian ocean water is strongly reduced (NOAGU). The control run is the same as discussed in HH2005 and HET2008. At the lateral boundaries the isopycnal layer thickness, including the mixed layer depth, are relaxed toward the density profiles obtained from Levitus et al. (1998). Also salinity is restored at the lateral boundaries. The Levitus data have also been used to initialize the ocean model. The experimental set-up of the NOAGU run is the same as for the CONTROL run. The only difference is that at the eastern lateral boundary at the southern tip of Africa density and salinity are now restored to values obtained from a global MICOM run with the same resolution and parameterizations, but forced with the CORE surface fluxes (Large and Yeager 2004). This MICOM run is characterized by a collapsed MOC due to insufficient deep-water formation in the North Atlantic. Most of the ocean-ice models forced by the CORE fluxes show an MOC collapse, which is probably due to too high freshwater fluxes in the Arctic (Griffies et al. 2008). Although this run suffers from the inability to simulate an MOC in accordance with the observations, it serves our goal to provide boundary conditions for a run with reduced Indian Ocean inflow. The main reason for taking the CORE run to modify the lateral boundary

conditions at southern tip of Africa is that it provides us with a coherent estimate of how the temperature and salinity characteristics of the water masses in MICOM would be affected due to a shut down of the Agulhas leakage. Apart from the different eastern lateral boundary conditions at the southern tip south of Africa, the experimental set-up of the NOAGU run is exactly the same as for the CONTROL run. Because the lateral boundary conditions are only changed at the southern tip of Africa (Fig.1), both runs feature a MOC of similar strength; the amplitude of the MOC is determined by the relaxation towards Levitus data at the southern boundary and the implied upwelling.

The boundary conditions for temperature and salinity in the NOAGU experiment are represented in Fig. 1, which shows the ocean model domain, the region where the conditions were applied and vertical profiles of the differences of temperature (T) and salinity (S) between NOAGU and CONTROL, along the oceanic portion of the easternmost oceanic boundary (20°E). These boundary conditions can be interpreted as prescribing an inflow of cold and fresh anomalies into the South Atlantic. The maximum amplitude of these perturbations are 4°C and 0.5 PSU. Starting from the control state, the model with the new boundary conditions was run for 50 years. In the following section we analyze the results considering how the anomalies propagated into the South Atlantic and affected the oceanic and atmospheric circulation.

3. Results

3.1 The Time Evolution of the Signal in the Ocean

After running the model with the no-Agulhas boundary conditions for one month, the plots with the differences in temperature and salinity with respect to CONTROL show a small plume of colder and fresher water near the southeastern corner of the domain (Fig. 1). As time goes on, the anomalies are advected into the South Atlantic by the ocean currents. Simultaneously the cooler temperature at the surface cools the atmosphere, which, by its turn advects the signal to the north-west by the trade winds. Due to this interaction with the atmosphere, the temperature anomaly in the mixed layer decreases rapidly downstream from the Agulhas retroflection region. The salinity anomaly, however, is not damped by the atmosphere and therefore persists much longer. It is clearly detectable in the mixed layer far away from the source.

The propagation of the anomalies from east (E) to west (W) is shown by the Hovmöller diagrams of Fig. 2, which represent the space-time evolution of the anomalous temperature

and salinity during the first 120 months of the NOAGU run along the path indicated in the box. In the Hovmöller diagrams the horizontal axis represents the points numbered from 1, in the Agulhas retroflection region, to 115, in the eastern equatorial Atlantic. The vertical axis indicates the months from the beginning of the run. Starting at the lower right corner, the anomalies reach the western boundary (W) in approximately 7 to 8 years after the interruption of the Agulhas leakage. Beyond this point, along the Brazilian coast and the Equator, the propagation is much faster, taking less than a year for the signal to reach the eastern equatorial Atlantic. The dashed vertical line in the Hovmöller diagrams represents the western boundary point W (38°W,15°S). In the mixed layer, the Hovmöller diagram for temperature shows that the signal is weakened before reaching the middle of the basin between Africa and South America. For salinity, however, the signal persists till reaching the westernmost point (W) of the diagonal line. Within the thermocline, both signals propagate all the way to the western boundary and on to the equatorial region, although the signal is substantially reduced before reaching the equator. These results, especially the clear appearance of the signal along the equator in the thermocline, corroborate with those of Hazeleger et al. (2003b), who used a Lagrangian trajectory technique. They confirm that MOC water is ventilated in the EUC.

3.2 The Final Ocean State

Figure 3 shows horizontal maps of the differences between NOAGU, averaged over the last decade of the 50-years of the NOAGU run, and the CONTROL climatology, for temperature and salinity in the mixed layer and in the thermocline between σ_θ=26.18 (layer 8) and σ_θ=27.22 (layer 12). In the mixed layer, the cold temperature anomaly decreases along the path followed by the Benguela and South Equatorial Currents. A slight warming is observed in the equatorial region and in the western half of the basin, south of 20°S. This warming is caused by changes in the atmospheric circulation and will be discussed in section 3.4.

The salinity pattern shows an overall freshening of the South Atlantic south of 20°S. The area affected by the salinity anomaly is much larger than for the temperature, because of the exchange of heat with the atmosphere which damps the temperature anomaly. However, in the tropical South Atlantic, between 10°S and 20°S, there is a band of positive salinity anomalies, which extends all the way from South America to Africa (top-right panel of Fig. 3).

Vertical profiles of salinity in that region (not shown here) reveal that the salinity anomaly is confined to the mixed layer. This suggests that this anomaly is due to an increase in the evaporation minus precipitation (E-P) fluxes resulting from changes in the atmospheric circulation. This will be further discussed in the section 3.4.

Within the thermocline (lower panels of Fig. 3), it is quite clear that both cold temperature (T) and fresh salinity (S) signals reach the Equatorial Under Current (EUC) and are advected eastward. From the equatorial region they are advected northward by the NBC into the North Atlantic. Finally we draw attention to the cooling and freshening observed in the Tropical North Atlantic, centered around the Guinea Dome, from the surface down to the thermocline. We will comment on that later.

The vertical structure of temperature and salinity anomalies along 30°W after 50 years of the NOAGU run is shown in Fig. 4. It reveals that south of 20°S the temperature signal is confined within the thermocline, whereas the anomalous salinity signal is also visible in the mixed layer. At about 15°S and 150 m depth a strong anomalous warm and saline signal is observed, which is not seen in the isopycnal layers (Fig. 3c,d). It is located beneath the positive salinity anomaly in the mixed layer. This anomalous saline and dense water in the mixed layer is associated with downwelling of the isopycnals, which is clearly seen in the increased depth of the isopycnal surface of σ_θ=26.18 (Upper black lines in Fig.4). This results in strong positive signals at the thermo- and halocline if z is used as vertical coordinate as in Fig. 4. In the equatorial region the cold and fresh anomalies in the EUC are clearly seen. Much weaker signals of T and S are observed in the mixed layer. For T even a slight warming is observed which will be discussed later. Similar as Fig. 3, Fig. 4 also shows that the signal propagates northward of the equator where it upwells around 15°N in the region of the Guinea Dome. The vertical profile of T and S along the Equator, shown in Fig. 5, confirms that the thermocline gets cooler and fresher and that the mixed layer is also freshened in the NOAGU experiment, without hardly any change in the temperature. An interesting feature is a pronounced warming seen at the bottom of the mixed layer in the eastern Atlantic. In the same region the freshening is reduced. The mechanisms that generate this response will be discussed in section 3.4.

As stated before the temperature and salinity anomalies are significantly affected by the changes in the atmospheric circulation. In the next section (3.3) we will describe these changes and subsequently investigate in section 3.4 the impact of the atmospheric response on the ocean circulation and the T and S distribution.

3.3 The Atmospheric Response

Due to the heat gained from the atmosphere, the cold SST anomaly is damped out downstream from the source. Consequently the air temperature distribution presents a similar pattern with cooling in the Agulhas region. In addition to the local cooling due to the heat loss to the ocean, the cooler air is advected to the northwest by the south-east trades. The result is a cool temperature stripe in the surface air temperature (SAT), extending northwestward across the subtropical South Atlantic (not shown). The increased meridional temperature gradient resulting from the cooler South Atlantic displaces the ITCZ northward, resulting in decreased precipitation in the tropical South Atlantic and more precipitation in the equatorial region, as indicated by the wind and precipitation anomaly patterns depicted in Fig. 6. These changes are in line with the results of Haarsma et al. (2003), where the impact of the South Atlantic SST dipole on the atmospheric circulation was investigated. In addition, the South Atlantic subtropical high is weakened, inducing anomalous westerly surface winds around 20°S and 20°W.

An interesting question can be raised with regard to the time lag of the atmospheric response in the equatorial region. As seen in Fig. 2, the oceanic signal takes 7 to 9 years to reach the equatorial Atlantic. Is that the same time scale of the atmospheric response in that region or does the anomalous signal go faster in the atmosphere? The response in the wind stress, shown in Fig. 6, is characterized by an increase of westward wind stress over the western Atlantic at the coast of the north eastern Brazil, and by an increase of northward wind stress over the eastern tropical Atlantic. The time evolution of the area averaged magnitude of the wind stress over these two regions is shown in Fig. 7. Notwithstanding the strong interannual variability it is seen that the atmospheric signal starts to affect the equatorial region after 3-5 years, well before the oceanic signal reaches that region, which is after 7-8 years (Fig. 1). The impact of that atmospheric signal on the ocean will be discussed below.

3.4 Impact of atmospheric response on the ocean

The atmospheric response affects the ocean circulation and the T and S distributions. A striking feature of the final oceanic state is that in the equatorial Atlantic, in spite of the cooling of the thermocline, the temperature of the mixed layer is practically not changed but

shows a slight warming instead (Fig. 3a). A notable warming is observed just above the thermocline (Fig. 5a). To further analyze this warming we have analyzed the heat budget of the mixed layer. Figure 8 shows the anomalous surface heat flux. It reveals that in the tropical Atlantic heat is lost from the mixed layer to the atmosphere. In a steady state this heat loss of the mixed layer must be compensated by anomalous diffusion, horizontal advection and vertical entrainment of heat. Analysis of the heat budget of the mixed layer in the model reveals that of these processes vertical entrainment is most important. This implies that the mixed layer is warmed, or less cooled from below and that the anomalous heat is subsequently released to the atmosphere. The signal is largest between 15°W and 0°E, and 1°S and 3°N.

A possible explanation of the warming of base of the mixed layer/upper thermocline can be that the atmospheric response, with a northward shift of the ITCZ, affects the equatorial Ekman divergence and vertical entrainment. The change in vertical velocity $w_e = -\nabla.(uh)$ at σ_θ=26.18, (location of the upper thermocline) is shown in Fig. 9a. It reveals anomalous downwelling (reduced upwelling) along the equator in the eastern Atlantic. This agrees with the anomalous downwelling due to the change in Ekman pumping as estimated from the change in the wind stress using equation (4) of Haarsma et al. (2005), where the damping timescale due to linear friction was taken to be five days (Fig. 9b). Because of the climatological vertical temperature gradient, with warm surface waters overlying a cold thermocline, this anomalous downwelling induces a warming of the mixed layer because it reduces the net upwelling of cold water into the mixed layer. The change is most notable at the top of the thermocline, where the vertical temperature gradient is largest. This is clearly seen in Fig. 5a, which shows the largest warming just above the thermocline. The anomalous downwelling also affects the salinity distribution at the bottom of the equatorial mixed layer. Figure 5b shows around 10°W a region of enhanced salinity, resulting from the reduced upwelling of less saline waters from below the halocline into the mixed layer.

To further investigate the impact of atmospheric coupling on the final state of the ocean, we performed two idealized experiments in which the coupling between the atmosphere and the ocean model is changed. In both experiments we use the NOAGU boundary conditions. In one experiment (NOAGU_climwind) we replaced the wind (wind stress and wind speed) by which the ocean model is forced with the climatological wind produced by the CONTROL experiment. The turbulent surface heat fluxes, however, are still computed with bulk formulae using the actual winds. In this experiment the ocean dynamics

are forced by the winds from the CONTROL run, whereas the heat budget is calculated in the same way as in the NOAGU experiment. In the other experiment (NOAGU_climprec), the ocean model receives the climatological precipitation of the CONTROL run, but is in all other aspects similar to the NOAGU run.

The wind and precipitation fields applied as forcing in NOAGU_climwind and NOAGU_climprec consist of an annual cycle without daily fluctuations. This results in an unwarranted shift of the climatological state, due to absence of the nonlinear forcing of the short term fluctuations of wind stress and precipitation. To correct for this unwarranted shift, we also repeated the CONTROL experiment and forced it with the climatological winds (CONTROL_climwind) to compare it with NOAGU_climwind, and with climatological precipitation (CONTROL_climprec) to compare it with NOAGU_climprec. The results of NOAGU_climwind – CONTROL_climwind and NOAGU_climprec – CONTROL_climprec will henceforth be called the Climwind and Climprec experiments.

Figure 10 shows the temperature and salinity anomalies in the equatorial plane for the Climwind experiment. It reveals a strong reduction of the warming just above the thermocline and a freshening of the mixed layer compared to the NOAGU simulations shown in Fig. 5, thereby supporting our hypothesis with respect to the impact of anomalous Ekman pumping on the equatorial temperature and salinity distribution. Figure 10b clearly shows how the anomalous fresh water below the thermocline enters the mixed layer at the eastern boundary due to the strong upwelling, and is subsequently advected westward by the Equatorial Current. Also Fig. 10a shows signs of upwelling of cold water at the far eastern boundary into the mixed layer.

In Fig. 10a the warming at the base of the mixed layer is somewhat less than in Fig. 5a, but still significant. This warming is located just above where the largest cooling in the lower thermocline occurs. The cooling of the subsurface waters by the closing of the warm water path enhances the climatological vertical density gradient of light warm water overlying dense cold water. This reduces the entrainment of cold water from below the thermocline into the mixed layer. The reduction of the diapycnal mass flux at the top of the thermocline is illustrated in Fig. 11. The net diapycnal mass flux consists of convection, diapycnal mixing and mixed layer entrainment/detrainment. Positive numbers denote an upward flux. From Fig. 11b,d one can see that at the top of the thermocline the mass flux is negative. There is a flux of mass from the thermocline into the mixed layer (the mixed layer deepens) in the region where also the anomalous warming is observed in the NOAGU run (Fig. 5a). This mass flux

compensates the mass loss in the mixed layer due to the Ekman pumping (upwelling). In the NOAGU run the diapycnal mass flux is reduced, as is the Ekman pumping (Fig 11a,c). So, reduced mixing of colder thermocline water into the mixed-layer leads to warming at the base of the mixed layer. After this water is detrained a warm anomaly occurs in the top of the thermocline, just below the base of the annually averaged mixed layer.

The slight warming in the western half of the basin south of 20ºS (Fig. 3b) disappears in the Climwind experiment, indicating that this warming is due to a reduction of the cooling by the trade winds resulting from a weakening of the subtropical high. The anomalously high salinity area at 10°S in Fig. 3b is located in the region of reduced precipitation due to the northward shift of the ITCZ (Fig. 6). This anomalous increase in salinity is only observed in the mixed layer. In section 3.2 we suggested that this salinity anomaly was due to the northward shift of the ITCZ. This is indeed confirmed by the Climprec experiment, revealing that the area of enhanced salinity almost completely disappears when the climatological precipitation field is used (not shown).

In both experiments with reduced atmospheric feedbacks, the mixed layer in the Guinea Dome region presents little changes as compared with the fully coupled run. This is an indication that the anomaly in that region is due to changes in the ocean circulation. In the whole South Atlantic, cold and fresh water from the thermocline is advected into the mixed layer. But the stable atmospheric boundary layer in the subtropics prevents that this anomaly is as strongly damped in the Guinea Dome as in the equatorial region of the ITCZ.

4. Summary and Conclusions

Using Speedy-MICOM we have investigated the impact of a shut down of the Agulhas leakage of Indian ocean water on the South and Tropical Atlantic climate and its variability. We have done this by analyzing the differences between a CONTROL run forced with Levitus (1998) data at the northern and southern boundary of MICOM, and a NOAGU run, in which the conditions at the open part of the eastern boundary, south of the southernmost tip of Africa, were replaced by values from an experiment with a collapsed MOC.

A shut down of the warm water path results in cold temperature and fresh salinity anomalies that propagate into the South Atlantic and eventually reach the equatorial region,

mainly in the thermocline. In the ocean, the time scale for the signal to arrive in the equatorial Atlantic is in the order of 7-8 years. After 50 years of simulation, there is an overall cooling and freshening of the South Atlantic, which causes a northward shift of the ITCZ. The resulting changes in the trade winds lead to reduced Ekman pumping in the equatorial region, which causes an increase of T and S at the top of the thermocline, and a slight increase in the mixed layer. Decreased entrainment of thermocline waters by reduced Ekman pumping in the Cold Tongue region is associated with an enhanced vertical stability due to the cooling of the thermocline. The anomalous signal in the Cold Tongue Area is transported by the Equatorial Undercurrent and subsequently spreads away from the Equator, within the thermocline. Part of this anomalous signal eventually reaches the Tropical North Atlantic, where it affects the Guinea Dome. In the atmosphere, the simulation's northward shift of the ITCZ is associated with a band of negative precipitation anomalies and higher salinities over the Tropical South Atlantic.

We have studied here the initial phase of a shut down of the warm water path: the advection of the signal into the tropical region, its interaction there with the atmosphere and the further northward spreading into the subtropical North Atlantic. The experimental set up, in which the MOC is not affected by the shut down of the warm water path, and in which the inflow of warm and salty Indian ocean water is replaced by an equal amount of fresh and cold Southern ocean water, is only valid in the initial phase of the shut down. The experiment should therefore be considered as a sensitivity experiment. An important result is that in the tropics, due to reduced Ekman pumping and enhanced vertical stability, the entrainment of cooler and fresher thermocline water is diminished. This means that the signal is partly preserved and advected farther northward where it eventually reaches the areas of deep water formation.

It is hypothesized from paleo data and simplified models (Weijer et al. 1999, Peeters et al., 2004) that the shut down of the Agulhas eventually affects the deep water formation in the North Atlantic and modifies the MOC. Our results support this hypothesis. It also reinforces the notion that the Agulhas leakage is a sensitive parameter for Atlantic decadal climate variability. A recent study by Biastoch et al. (2008) suggests in an ocean only experiment that decadal variability of the MOC is related to variability of the Agulhas leakage. Our results support that hypothesis because it indicates that the modified water mass characteristics in the South Atlantic due to variations in the Agulhas leakage are preserved when crossing the Atlantic. This is a prerequisite for the impact of variations in Agulhas leakage on the deep

water formation that drive the variations in the MOC. The results of this study also show that the initial response to the closing of the Agulhas leakage (cooling of the South Atlantic and northward shift of the ITCZ) is different from the final response after the MOC has collapsed (warming of the South Atlantic and a southward shift of the ITCZ (Haarsma et al. 2008)). This has implications for monitoring the South and tropical South Atlantic with respect to decadal variability and anthropogenic climate change and also for paleo research if the time resolution of the paleo data is sufficient high.

We realize the limitations of this study. The MOC is determined by the southern boundary conditions which allows an investigation of the effect of replacing Agulhas leakage by an import of Southern Ocean water. In addition the resolution of the ocean model is 1 degree which does not allow the simulation of mesoscale processes like formation of rings and filaments that play a crucial role in dynamics of the Agulhas leakage. Nevertheless, the CONTROL run features Agulhas leakage in the form of a steady current flowing into the South Atlantic. We do not think that these limitations affect the main results of this study: That the characteristics of the modified water masses largely remain unaffected when crossing the Atlantic making the Greater Agulhas System an important source region for climate change and decadal variability of the Atlantic.

The results and the limitations of our study therefore strongly suggest the need for a detailed analysis with a coupled ocean-atmosphere model in which the dynamics of Agulhas leakage is properly simulated.

Acknowledgments. This research is an activity of the South Atlantic Climate Change (SACC) consortium supported by the Inter-American Institute for Global Change Research (IAI), Project CRN2076. The IAI is supported by NSF grant GEO-0452325. The work was started during a three-month visit of R.J. Haarsma to IOUSP in 2006 and continued during a two-month visit of E. Campos to KNMI in early 2007. This exchange of visits was mainly supported by FAPESP (Grants 2005/04315-0 and 2006/03939-8). We also acknowledge the additional support from KNMI and CNPq, which provides a Research Fellowship to the second author (Proc. 307785/2004-1).

References

Biastoch, A., C.W. Böning and J.R.E. Lutjeharms (2008) Agulhas leakage dynamcis affects decadal variability in Atlantic overturning circulation. *Nature,* **456,** 489-492.

Bleck, R., C. Rooth, D. Hu and L.T. Smith (1992) Salinity-driven thermocline transients in a wind- and thermohaline-forced isopycnic coordinate model of the North Atlantic. *J. Phys. Oceanogr.,* **22,** 1486-1505.

Breugem, W.P., W. Hazeleger and R.J. Haarsma (2007) Multimodel study of tropical Atlantic variability and change. *Geophys. Res. Lett.,* **33,** L23706 doi:10.1029/2006GL027831

Chang, P., R. Zhang, W. Hazeleger, C. Wen, X. Wan, L. Ji, R.J. Haarsma, W.P. Breugem and H. Seidel (2008) An Oceanic Bridge Between Abrupt Changes in North Atlantic Climate and the African Monsoon. *Nature Geoscience* **1,** 444 – 448.

Dahl, K.A., A.J. Broccoli and R. Stouffer (2005) Assessing the role of North Atlantic freshwater forcing in millennial scale climate variability: A tropical Atlantic perspective. *Climate Dyn.,* **24,** 325-346.

Gordon, A.L. (1986) Interocean exchange of thermocline water. *J. Geophys. Res.,* **91,** C4, 5037-5046.

Griffies, S et al. (more than 8 co-auhors) (2008) Coordinated Ocean-Ice Reference Experiments (COREs). *Ocean Mod., **26,** 1-46, 2009.*

Haarsma, R.J., E.J.D. Campos and F. Molteni (2003) Atmospheric response to South Atlantic SST dipole. *Geophys. Res. Lett.,* **30**(16), 1864, doi:10.1029/2003GL017829.

Haarsma, R.J. E.J.D. Campos, W. Hazeleger, C. Severijns, A.R. Piola and F. Molteni (2005) Dominant modes of variability in the South Atlantic: A study with a hierarchy of ocean-atmosphere model. *J. Climate,* **18,** 1719-1735.

Haarsma, R. J., E.. Campos, W. Hazeleger and C. Severijns (2008) Influence or the Meridional Overturning Circulation on the Tropical Atlantic Climate and Variability. *J. Climate,* **21,** 1403-1416.

Hazeleger, W, C. Severijns, R.J. Haarsma, F. Selten, A. Sterl (2003a) SPEEDO-model

description and validation of a flexible coupled model for climate studies. KNMI, *Technical Report, TR-257, de Bilt, The Netherlands,* 37 pp.

Hazeleger, W., P. de Vries en Y. Friocourt (2003b) Sources of the Equatorial Undercurrent in the Atlantic in a High-Resolution Ocean Model . *J. Phys. Oceanography,* **33,** 4, 677-693, doi:10.1175/1520-0485

Hazeleger, W. and R.J. Haarsma (2005) Sensitivity of tropical Atlantic climate to mixing in a coupled ocean-atmosphere model. *Climate Dyn.,* **25,** 387-399, doi:10.1007/s00382-005-0047

Hazeleger, W. en S. Drijfhout (2006) Subtropical Cells and Meridional Overturning Circulation pathways in the tropical Atlantic. *J. Geophys. Res.,* **111,** doi: 10.1029/2005JC002942

Large, W.G. and S.G. Yeager (2004) Diurnal to decadal global forcing for ocean and sea-ice models: the data sets and flux climatologies,NCAR *Technical Note: NCAR/TN-460+STR,* CGD Division.

Levitus, S., T.P. Boyer, M.E. Conkright, T. O'Brien, J. Antonov, C. Stephens, L. Stathoplos, D. Johnson, R. Gelfeld (1998) NOAA Atlas NESDIS 18, WORLD OCEAN DATABASE 1998: Vol 1: Introduction. US Government Printing Office, Washington DC, 346 pp.

Molteni, F. (2003) Atmospheric simulations using a GCM with simplified physical parameterizations. I: model climatology and variability in multi-decadal experiments. *Climate Dyn.,* **20,** 175-191.

Peeters, F.J.C., R. Achinson, G.J.A. Brummer, W.P.M. de Ruijter, G. M. Ganssen, R.R. Schneider, E. Ufkes and D. Kroon (2004) Vigorous exchange between Indian and at the end of the last five glacial periods. *Nature* **430**, 661-665.

Peterson, L.C., G.H. Haug, K.A. Hughen, U. Röhl (2000) Rapid changes in the hydrological cycle of the tropical Atlantic during the last glacial. *Science*, **290,** 1947-1951.

Rintoul, S.R. (1991) South Atlantic Interbasin Exchange. *J. Geophys. Res.,* **96** (C2), 2675-2692

Stott, L., C. Poulsen, S. Lund and R. Thunell (2002) Super ENSO and global climate oscillations at millennial time scales. *Science,* **297,** 222-226.

Vellinga, M. and R.A. Wood (2002) Global climatic impacts of a collapse of the Atlantic

thermohaline circulation. *Climatic Change,* **54,** 251-267.

Weijer, W., de Ruijter, W. P. M., Dijkstra, H. A., and van Leeuwen, P. J. (1999) Impact of interbasin exchange on the Atlantic overturning circulation, *J. Phys. Oceanogr.,* **29,** 2266–2284.

Xie, S.-P., and J.A. Carton (2004) Tropical Atlantic variability: Patterns, mechanisms and impacts. *Earth's Climate: The Ocean-Atmosphere Interaction, Geophys. Monogr.,* **Vol. 147**, Amer. Geophys. Union, 121-142.

Zhang, R., and T. L. Delworth (2005) Simulated tropical response to a substantial weakening of the Atlantic thermohaline circulation. *J. Climate,* **18,** 1853-1860.

Figure Captions

Fig. 1: Top two panels: Vertical profiles of the (**a)** temperature- [°C], and (**b**) salinity anomalies [PSU] used as forcing conditions on the southeastern boundary for the NOAGU experiments. These anomalies were obtained from a global run with a collapsed thermohaline circulation. Lower panel (**c**): Surface salinity anomaly one month after the start of the NOAGU run.

Fig. 2: Time history of the temperature (left panels) and salinity (right panels) anomalies along the path indicated in the small map in the center of the figure, for the first 10 years of the NOAGU simulation. The horizontal axis represents the points numbered from 1, in the eastern equatorial Atlantic, to 115, in the Agulhas Retroflection region. The vertical axis indicates the months from the beginning of the run. The dashed vertical line in each plot represents the western boundary point W (38°W, 15°S). Upper panels: mixed layer. Lower panels: averaged over the thermocline (between σ_θ=26.18 and σ_θ=27.22).

Fig. 3: Upper panels: temperature (**a**), and salinity (**b**) anomalies averaged over the last 10 years of the 50-years NOAGU run for the mixed layer. Lower panels: temperature (**c**), and salinity (**d**), vertically averaged over the thermocline (between σ_θ=26.18 and σ_θ=27.22).

Fig. 4: The vertical structure of temperature- (**a**), and salinity (**b**) anomalies along 30°W averaged over the last 10 years of the 50-years NOAGU run. The thick upper and lower black solid lines indicate the isopycnal surfaces of σ_θ=26.18 and σ_θ=27.22 respectively for the CONTROL run. The dashed lines as the solid lines, but now for the NOAGU run. The green line is the 20° isotherm of the CONTROL run.

Fig. 5: Vertical profiles of the temperature- **(a),** and salinity **(b)** anomalies averaged over the last 10 years of the NOAGU run along the equator averaged between 2°S and 2°N.

Fig. 6: Anomalous precipitation [mm day^{-1}] and wind stress [N m^{-2}] averaged over the last 10 years of the NOAGU run.

Fig. 7: Time evolution of the anomalous magnitude of the wind stress [N m^{-2}] of the NOAGU run averaged over the boxes 35°W - 15°W, 15°S – 5°S (thick solid line), and 10°W – 10°E, 0°N – 10°N (thick dashed line). The thin lines denote the means averaged over the last 45 years of the NOAGU integration for the respective boxes.

Fig. 8: Anomalous surface heat flux [W m^{-2}] (positive upward) averaged over last 10 years of the NOAGU run.

Fig. 9: Upper panel (**a**): Anomalous vertical velocity $w_e = -\nabla.(uh)$ at the isopycnal surface σ_θ=26.18 between the NOAGU and CONTROL run [10^{-6} m s^{-1}]. Lower panel (**b**): Estimated change in vertical velocity [10^{-6} m s^{-1}] due to a change in the Equatorial Ekman pumpingbetween the NOAGU and CONTROL run based on the simulated change in the equatorial wind stress and equation (4) of HH2005, with a linear friction of 5 days.

Fig. 10: Vertical profiles of the temperature**-(a)** and salinity **(b)** anomalies along the equator averaged between 2°S and 2°N for the Climwind experiment.

Fig. 11: Top two panels: (**a**) Anomalous diapycnal upward mass flux [10^3 m^3 s^{-1}] (NOAGU minus CONTROL), and (**b**) net upward diapycnal mass flux for the CONTROL run at the top of the thermocline (σ_θ=26.18), averaged over the last 10 years. Bottom panels: Vertical profiles of the upward diapycnal mass flux in the equatorial region for (**c**) NOAGU minus CONTROL, and (**d**) CONTROL. The lines labeled K=8 and K=12 represent the isopycnal surfaces σ_θ=26.18 and σ_θ=27.22.

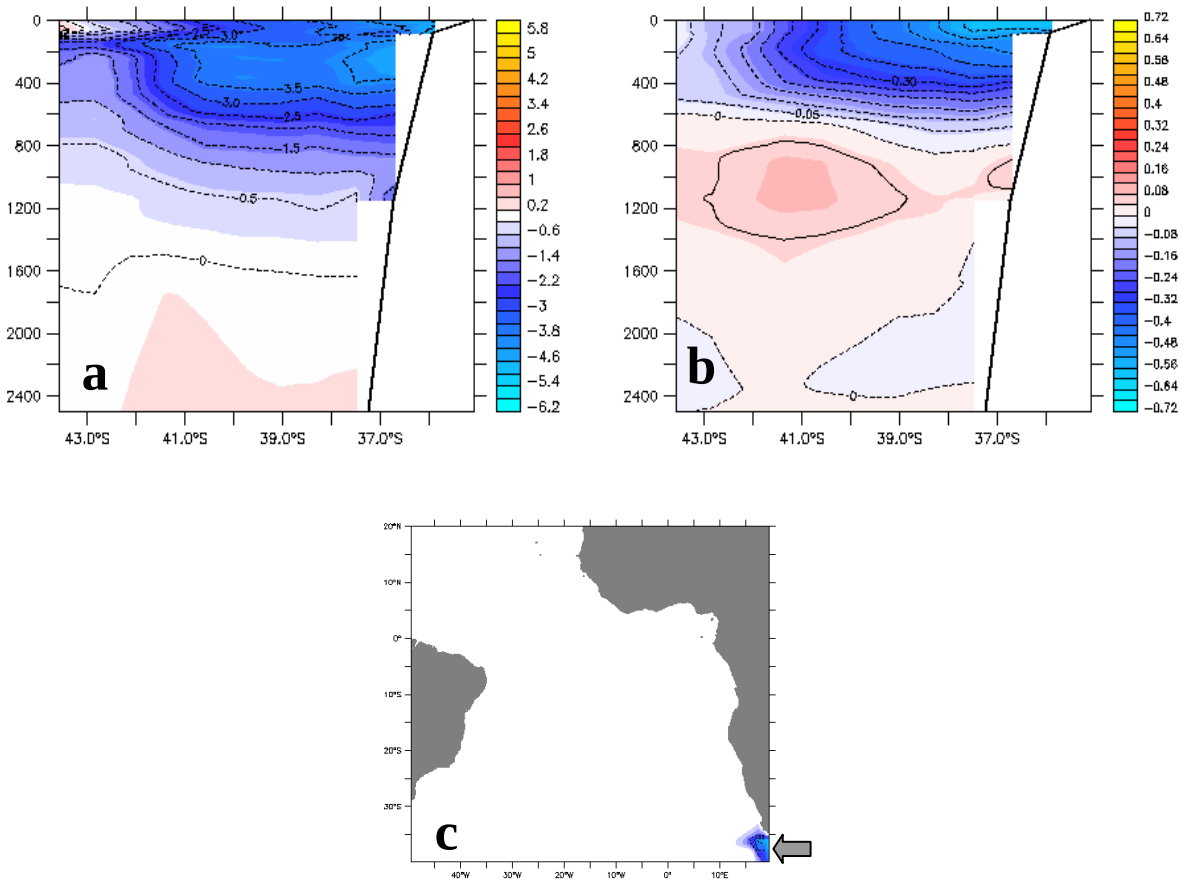
a
b
c
0
400
800
1200
1600
2000
2400
43.0°S
41.0°S
39.0°S
37.0°S
5.8
5
4.2
3.4
2.6
1.8
1
0.2
−0.6
−1.4
−2.2
−3
−3.8
−4.6
−5.4
−6.2
0.72
0.64
0.56
0.48
0.4
0.32
0.24
0.16
0.08
0
−0.08
−0.16
−0.24
−0.32
−0.4
−0.48
−0.56
−0.64
−0.72

FIG.1

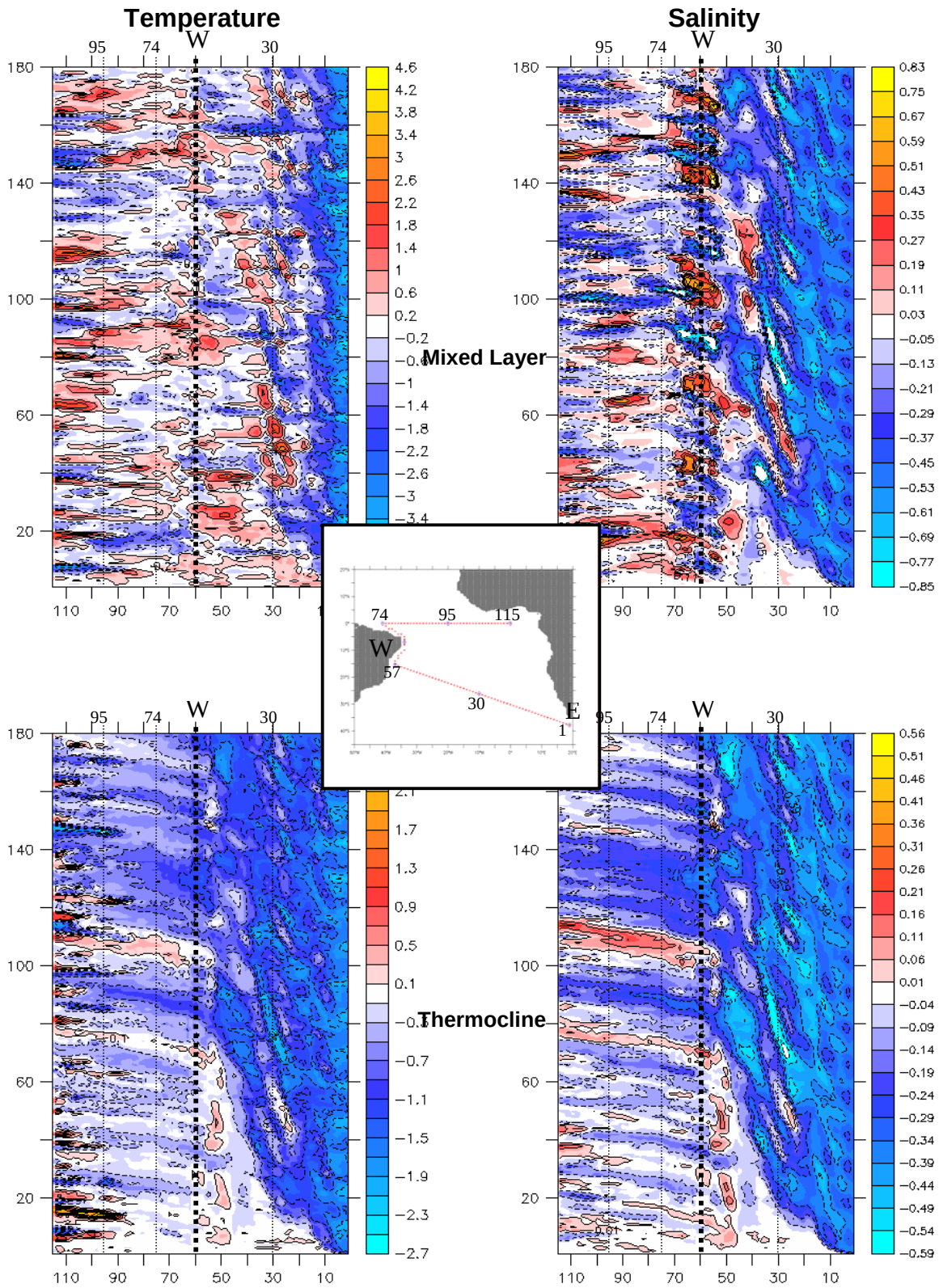
Temperature
Salinity
Mixed Layer
Thermocline
95
74
W
30
180
140
100
60
20
110
90
70
50
30
10
4.6
4.2
3.8
3.4
3
2.6
2.2
1.8
1.4
1
0.6
0.2
−0.2
−0.4
−1
−1.4
−1.8
−2.2
−2.6
−3
−3.4
0.83
0.75
0.67
0.59
0.51
0.43
0.35
0.27
0.19
0.11
0.03
−0.05
−0.13
−0.21
−0.29
−0.37
−0.45
−0.53
−0.61
−0.69
−0.77
−0.85
74
95
115
W
57
30
E
1
2.1
1.7
1.3
0.9
0.5
0.1
−0.3
−0.7
−1.1
−1.5
−1.9
−2.3
−2.7
0.56
0.51
0.46
0.41
0.36
0.31
0.26
0.21
0.16
0.11
0.06
0.01
−0.04
−0.09
−0.14
−0.19
−0.24
−0.29
−0.34
−0.39
−0.44
−0.49
−0.54
−0.59

Fig. 2

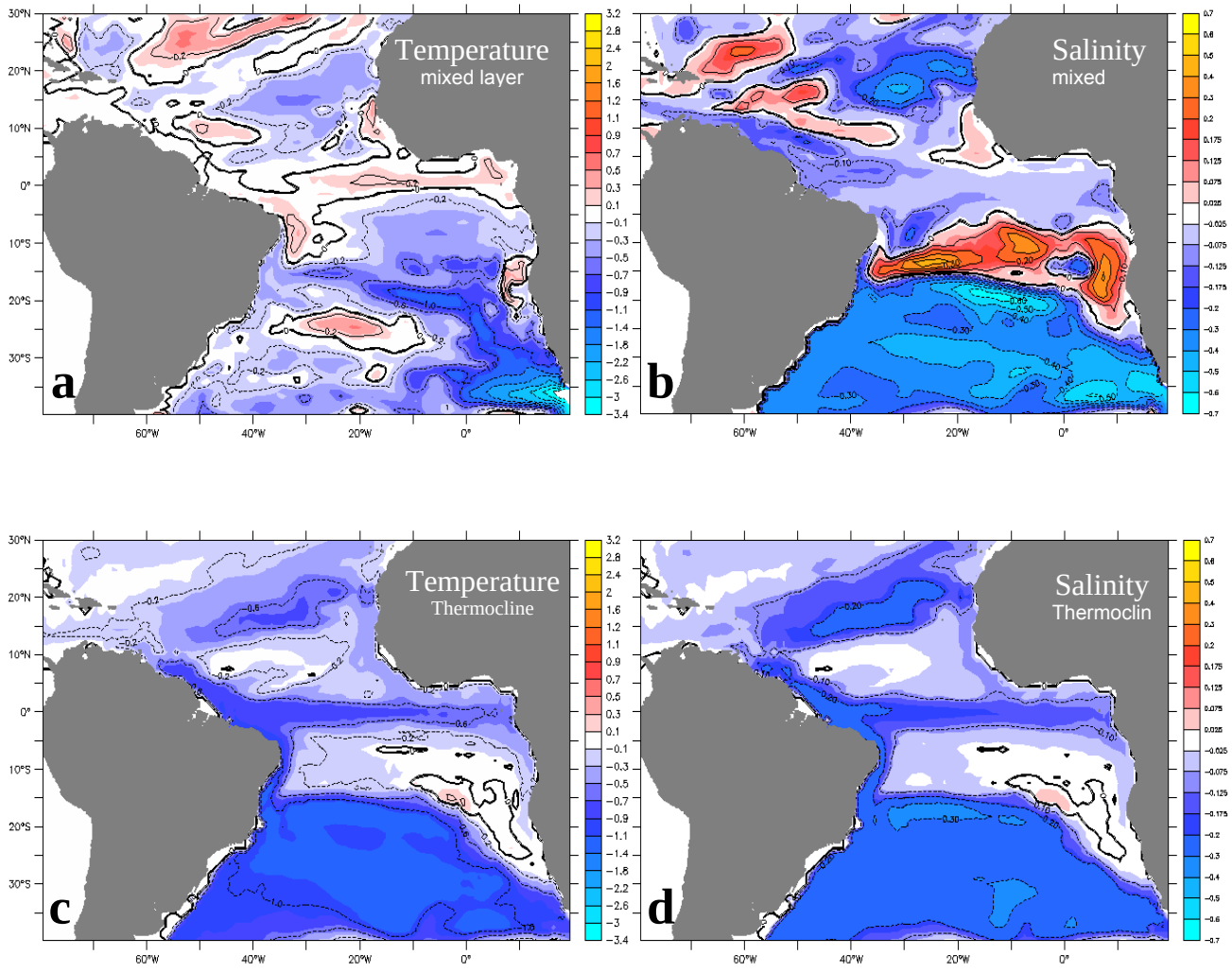
Temperature
mixed layer
a
Salinity
mixed
b
Temperature
Thermocline
c
Salinity
Thermoclin
d
30°N
20°N
10°N
0°
10°S
20°S
30°S
60°W
40°W
20°W
0°

Fig. 3

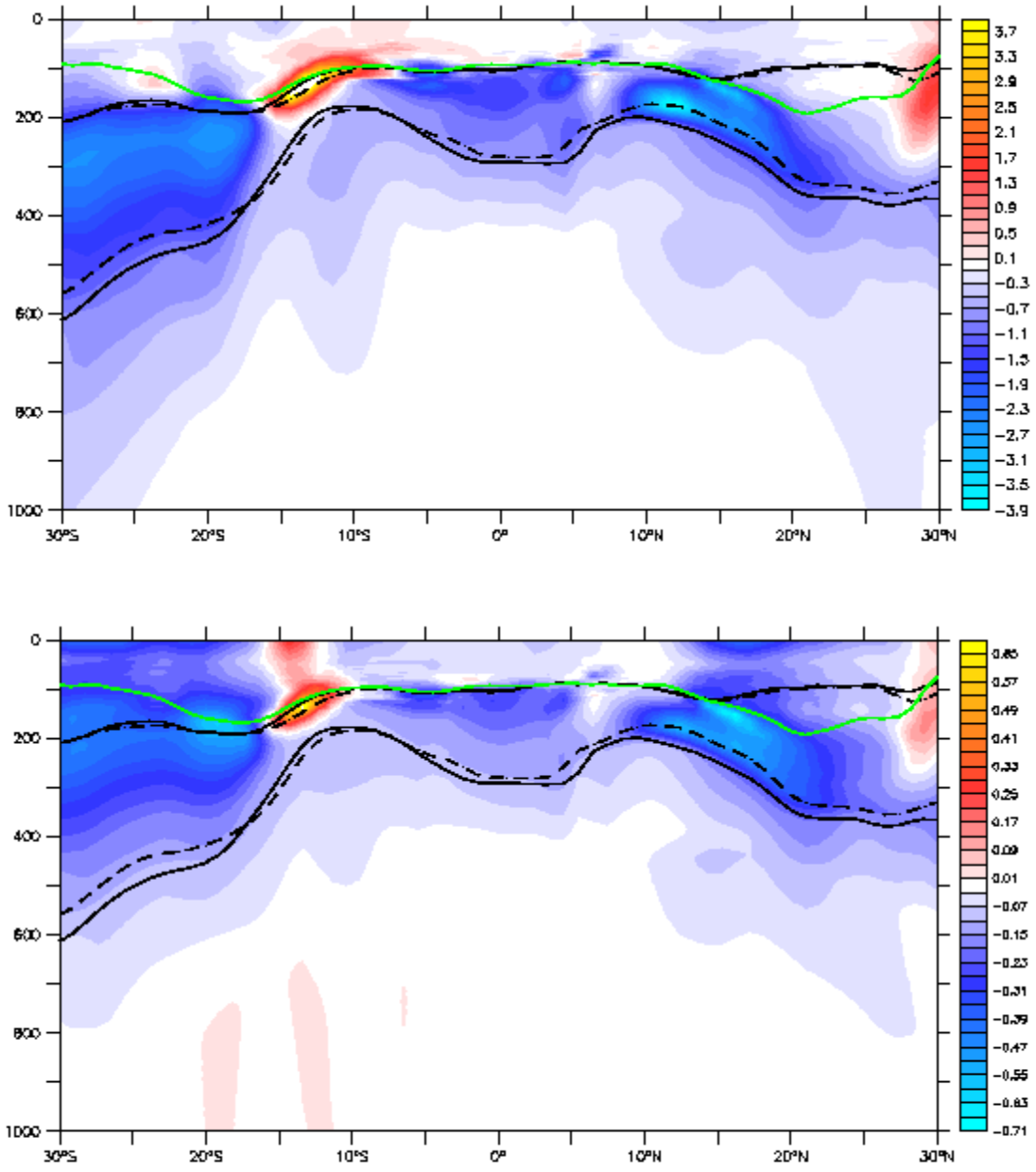
0
200
400
600
800
1000
30°S
20°S
10°S
0°
10°N
20°N
30°N
3.7
3.3
2.9
2.5
2.1
1.7
1.3
0.9
0.5
0.1
−0.3
−0.7
−1.1
−1.5
−1.9
−2.3
−2.7
−3.1
−3.5
−3.9
0.85
0.57
0.49
0.41
0.33
0.25
0.17
0.09
0.01
−0.07
−0.15
−0.23
−0.31
−0.39
−0.47
−0.55
−0.63
−0.71

Fig. 4

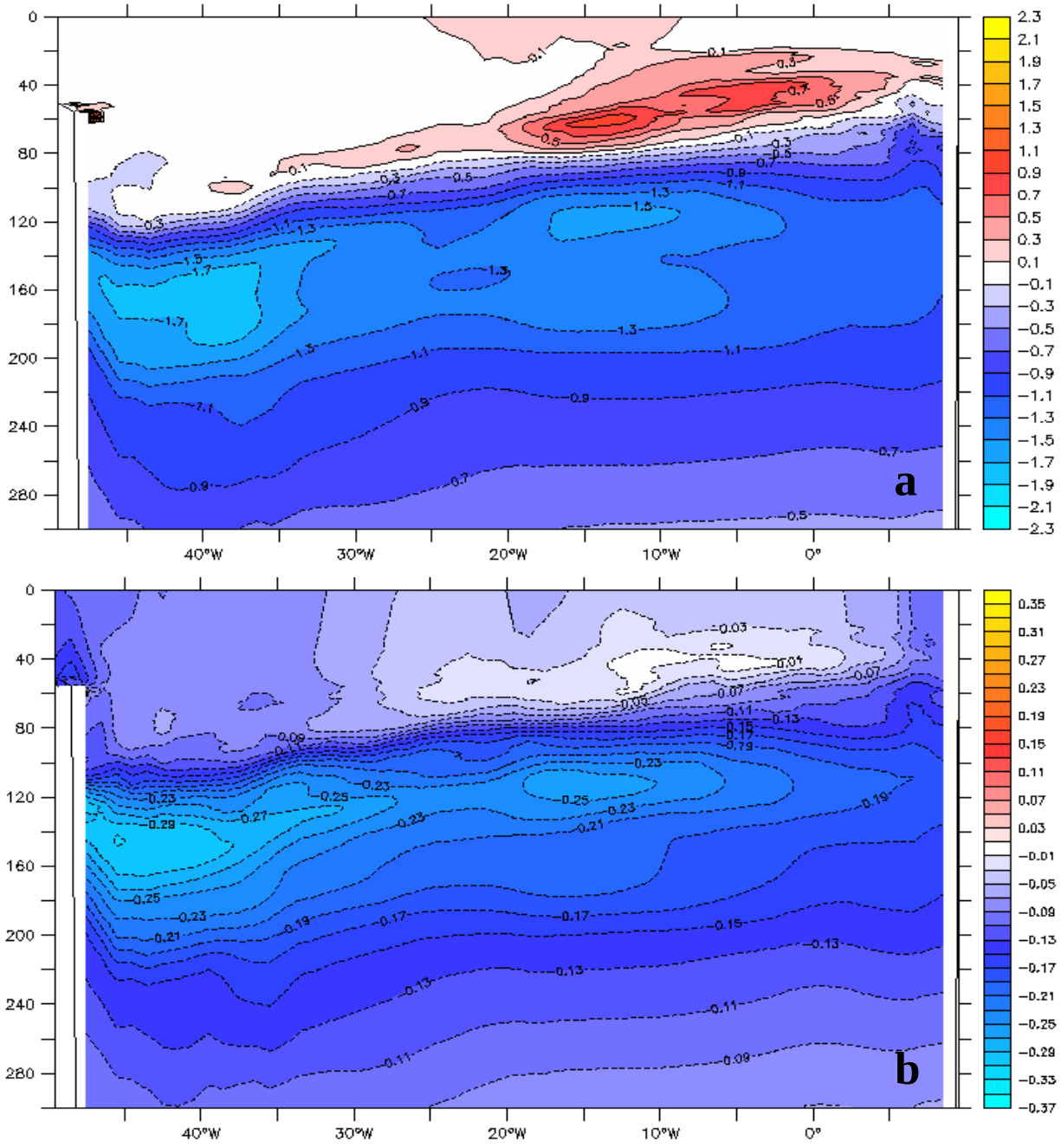

Fig. 5

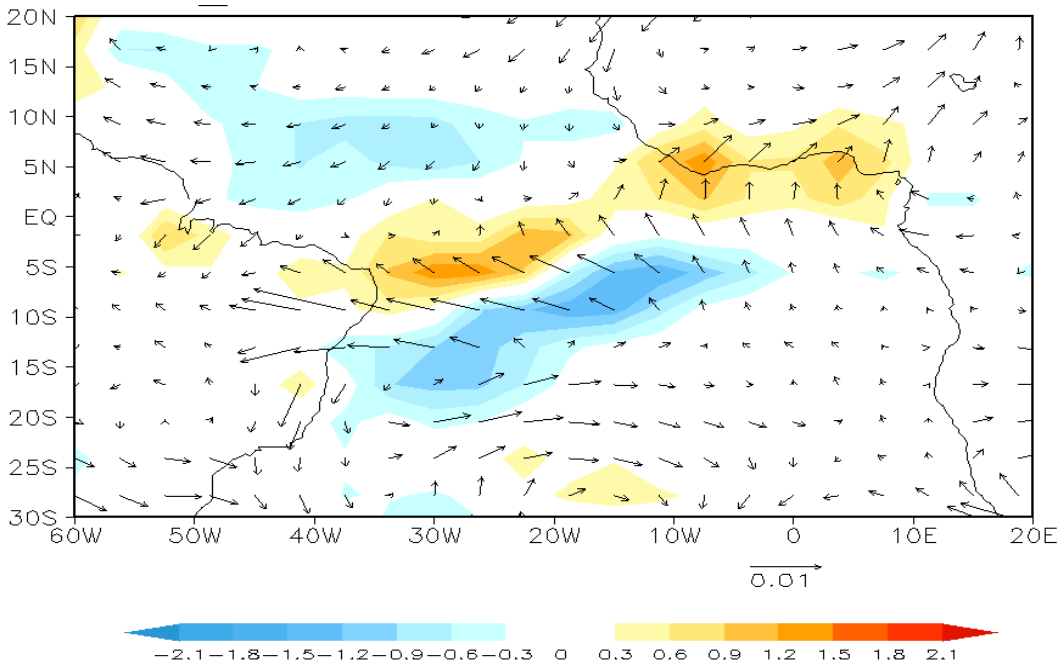
20N
15N
10N
5N
EQ
5S
10S
15S
20S
25S
30S
60W
50W
40W
30W
20W
10W
0
10E
20E
0.01
−2.1 −1.8 −1.5 −1.2 −0.9 −0.6 −0.3 0 0.3 0.6 0.9 1.2 1.5 1.8 2.1

Fig. 6

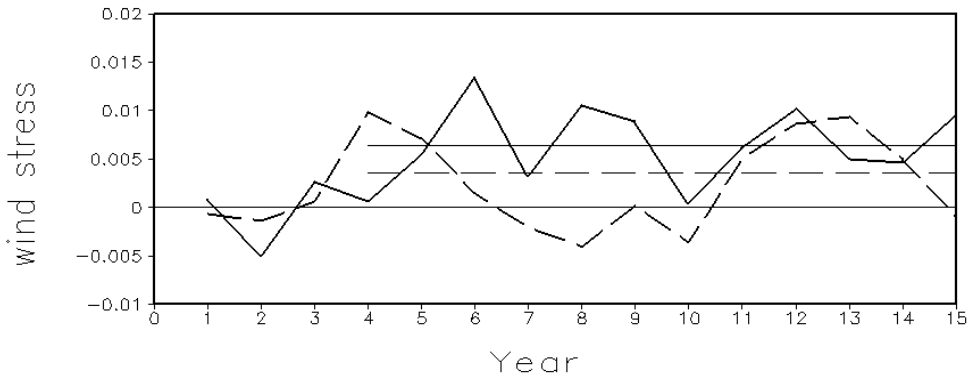
wind stress
0.02
0.015
0.01
0.005
0
−0.005
−0.01
0
1
2
3
4
5
6
7
8
9
10
11
12
13
14
15
Year

Fig. 7

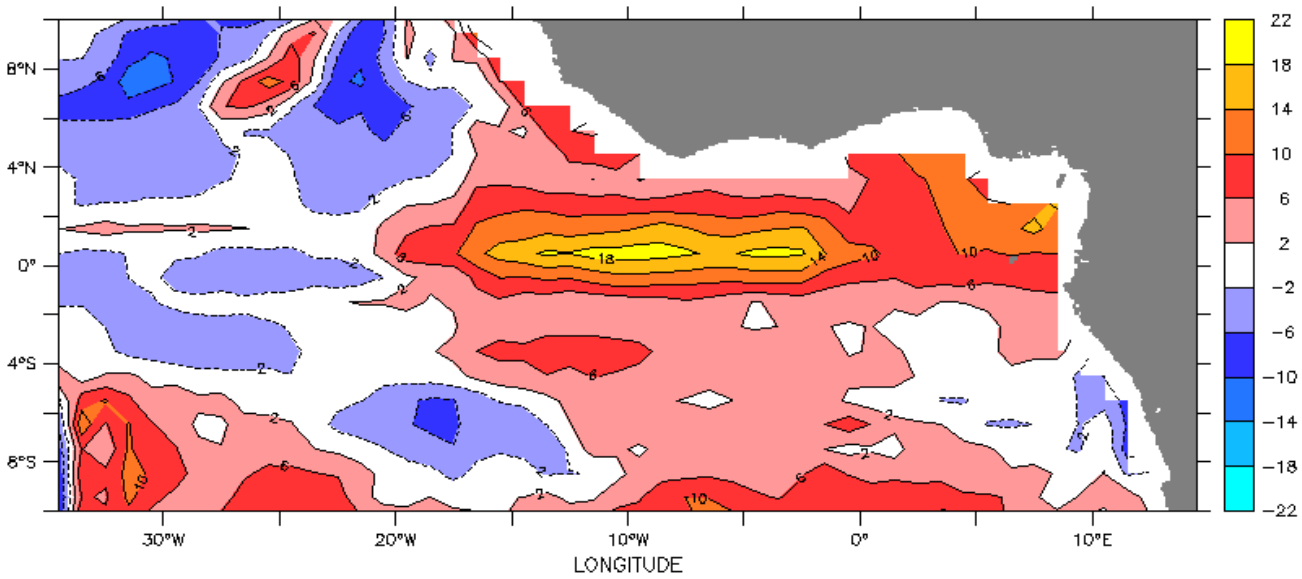
8°N
4°N
0°
4°S
8°S
30°W
20°W
10°W
0°
10°E
LONGITUDE
22
18
14
10
6
2
−2
−6
−10
−14
−18
−22

Fig. 8

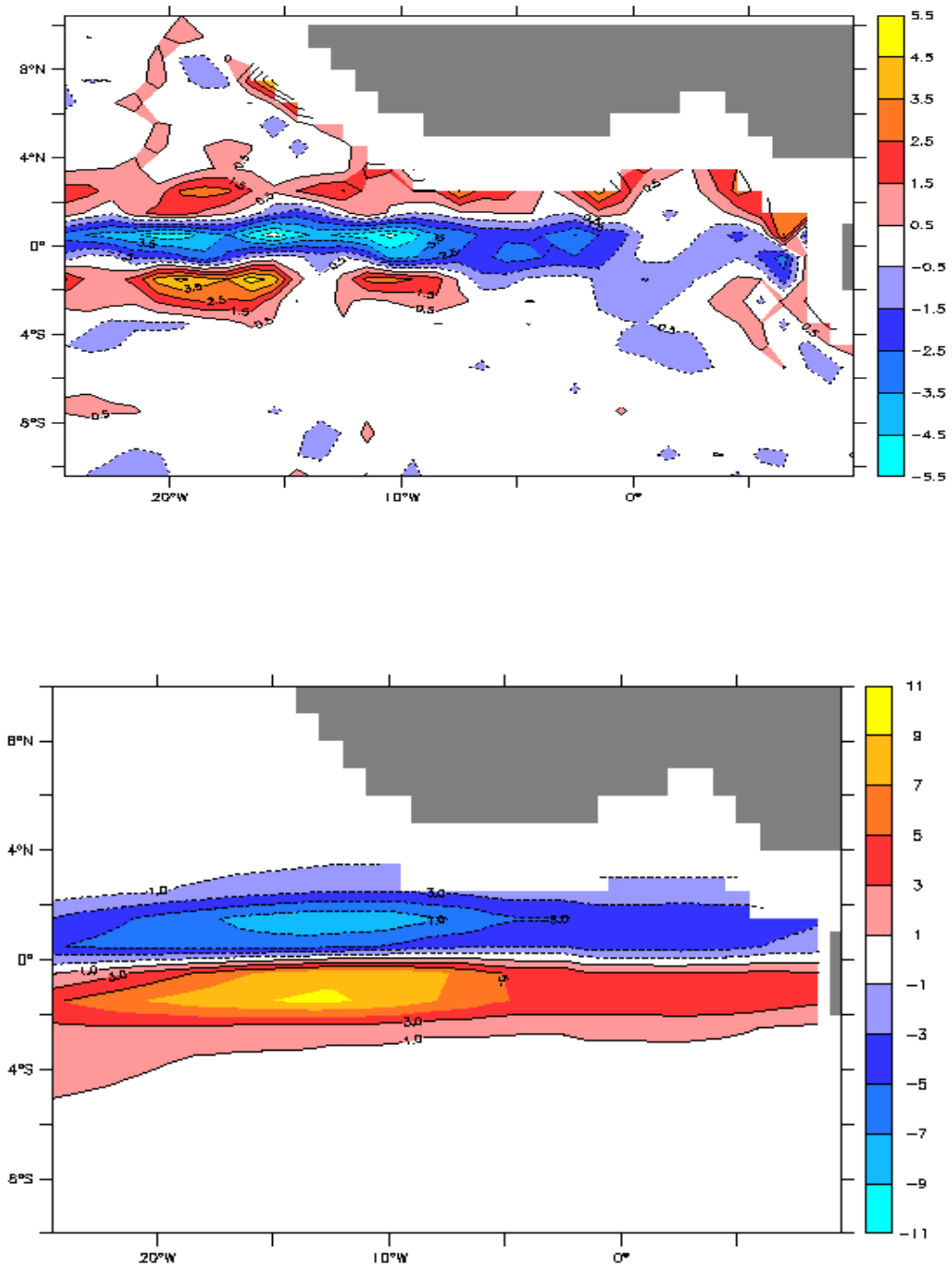
8°N
4°N
0°
4°S
8°S
20°W
10°W
0°
5.5
4.5
3.5
2.5
1.5
0.5
−0.5
−1.5
−2.5
−3.5
−4.5
−5.5
11
9
7
5
3
1
−1
−3
−5
−7
−9
−11

Fig. 9

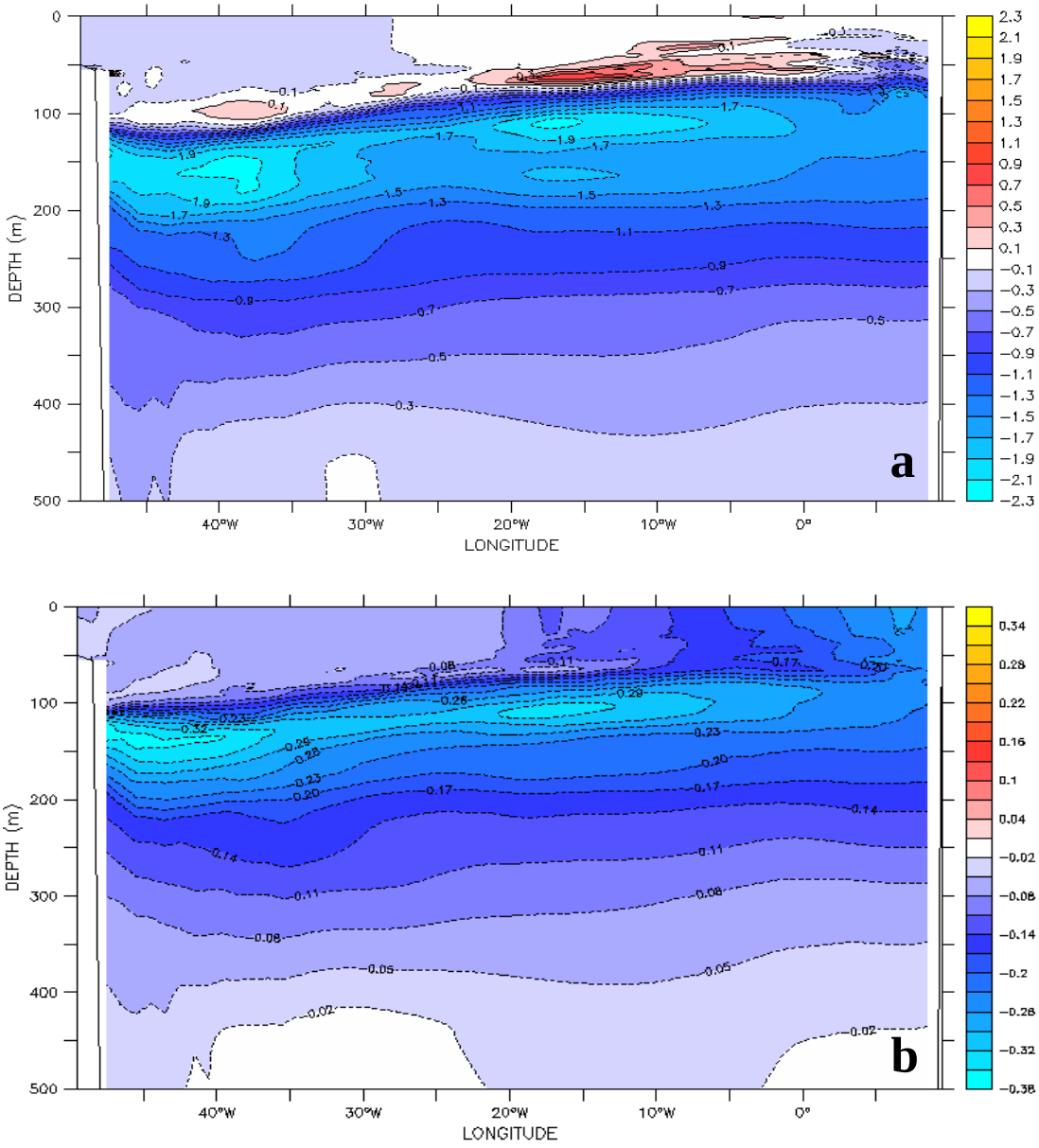

Fig.10

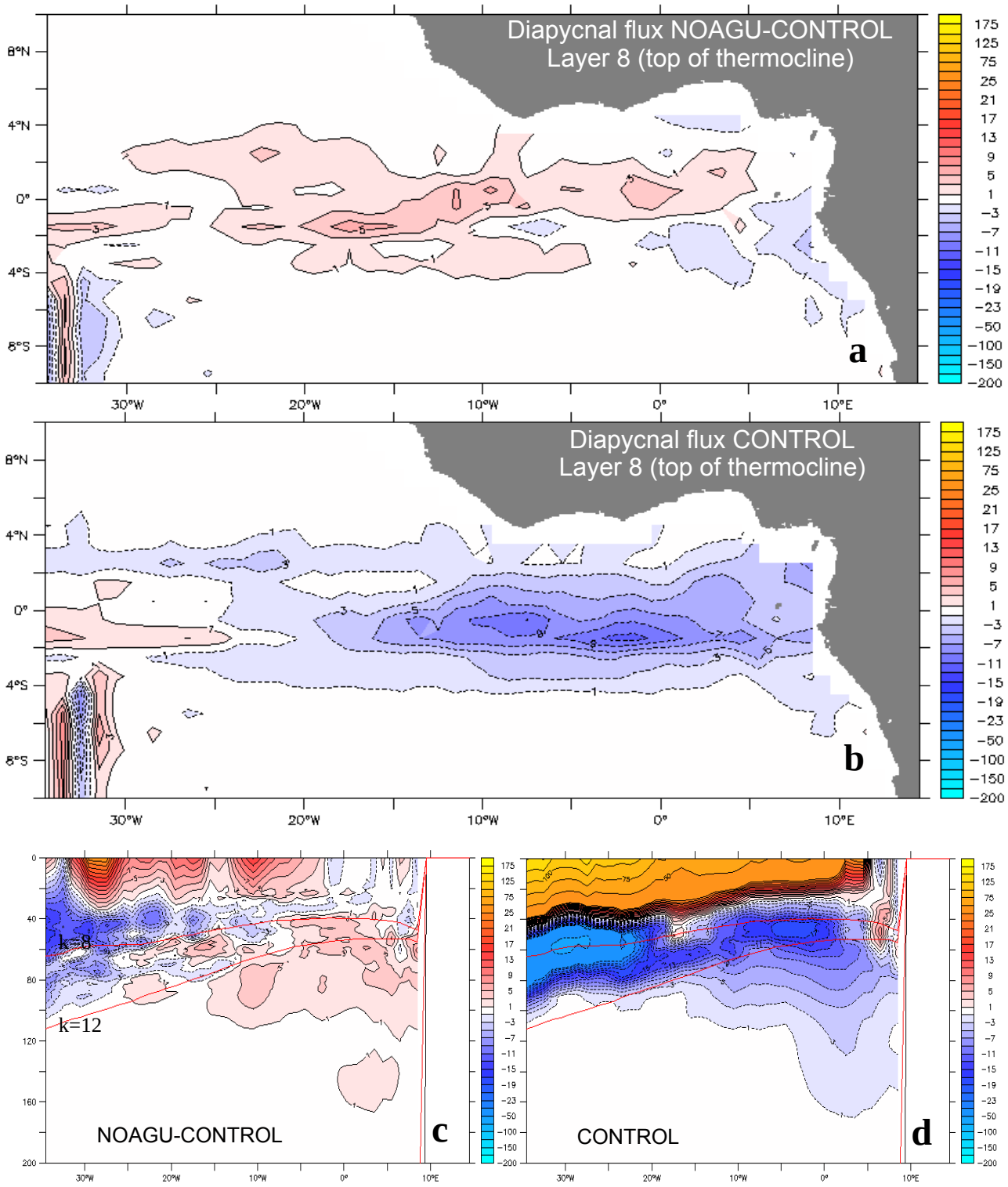
Diapycnal flux NOAGU-CONTROL
Layer 8 (top of thermocline)
a
Diapycnal flux CONTROL
Layer 8 (top of thermocline)
b
k=8
k=12
NOAGU-CONTROL
c
CONTROL
d

Fig. 11